Nanobiology (1993) 2, 55–63

STM Barrier-height Images and Topographic Images of Denatured DNA

CHUNLI BAI, DAWEN WANG, JIANGUO GU, CHANGCHUN DAI, JIAN YIE,* LISAN GONG* AND CIQUAN LIU**

Institute of Chemistry, Chinese Academy of Sciences, Beijing 100080, China

DNA helices can be denatured by being heated over their T_m *point. If cooled down quickly, most unraveled DNA strands cannot be reannealed and conformational variances could then be directly observed with scanning tunneling microscopy. In order to differentiate DNA molecules from graphite surface features, topographic and barrier-height images were acquired simultaneously. This paper presents scanning tunneling microscopic images of denatured lambda phage DNA. Unusual triple-stranded, braid-like and other variant conformations of denatured DNA were observed in air.*

INTRODUCTION

Scanning tunneling microscopy (STM), being an excellent probing tool for studying topographic and electronic properties of many surfaces on the atomic scale, has been used to study biological materials under different environments. The direct observations of B, A, Z-form DNA have already been performed by STM (Arscott *et al.*, 1989; Beebe *et al.*, 1989; Dunlap & Bustamante, 1989; Lee *et al.*, 1989; Lindsay *et al.*, 1989; Driscoll *et al.*, 1990). It has been known that the DNA conformations may be varied in different environments or treated by different physical and chemical methods. However, the detailed variations currently are not well known. Using STM, it may be possible to image these variant conformations of DNA and provide new information.

DNA can be denatured by being heated over its T_m point. If cooled down quickly, most of the denatured DNA strands cannot be reannealed and would result in conformational variances. In this paper, we present some STM images showing these variant conformations of DNA, which include the direct observations of a triple-stranded, braid-like conformation and joint structures of triple-stranded, braid-like segments and right-handed double helical segments.

The application of STM to biological materials requires the samples to be placed on conductive surfaces. The substrates must have a vertical roughness smaller than the vertical dimension of the sample. They also must have moderate interactions with the biological molecules in order to avoid the destruction of the integrity of the sample, and prevent the displacement of the sample by the mechanical and electrical forces exerted by the tunneling

*Present address: South China Normal University, Guangzhou 510631, China. **Present address: Kunming Institute of Zoology, Academia Sinica, Kunming 650107, China.

tip as it scans the sample. From these considerations, graphite and gold are suitable for using as conducting substrates. Unfortunately, some researchers (Sommerfeld *et al.*, 1990; Clemmer & Beebe, 1991) presented some images of highly oriented pyrolytic graphite (HOPG) and gold surface features which may be confused with that of biological materials. Therefore, it is imperative when applying STM to biological materials that an effective experimental method be established for distinguishing the biomolecules from the artefacts of substrates. Allison *et al.* (1990) have used scanning tunneling spectroscopic (STS) images to differentiate DNA molecules from graphite artefacts based on the spectroscopic images of DNA showing contrast due to local conductivity variations. We have found that it is also possible to distinguish DNA images from graphite surface features by use of barrier-height measurement because the barrier-height images of graphite features show no remarkable corrugations compared to those of biomolecules under the same experimental conditions.

EXPERIMENTS

The STM experiments were performed in air with home-made STM apparatus (Bai, 1989) using a mechanically prepared Pt/Ir (80%/20%) tip. A small voltage modulation was superimposed on the *Z*-axis voltage at a frequency of about 15 kHz, which is too fast for the feedback circuit to follow. The dI/dS, measured with phase-sensitive detection of the current at the modulation frequency, is directly related to the square root of the local barrier-height according to the simple model currently utilized to relate the tunneling current to the gap distances and the barrier height.

Lambda DNA–Hind III was produced by Sino-American Biotechnology Company (fragment sizes (bp): 23130, 9416, 6557, 4361, 2322, 2027, 564, 125). SDS-PAGE and HPLC analyses were performed to assay for purity. The results of SDS-PAGE showed that when the content of individual protein involved in Dalton Mark VII-L was more than 100 ng, their bands can be observed under our experimental conditions using silver stain. While the total load of lambda DNA–Hind III in SDS-PAGE was 8975 ng, no protein bands were detected in the range of low molecular weight. This suggested that the content of proteins involved in the sample was less than 1.2%. The lambda DNA–Hind III sample was hydrolyzed in 6N HCl solution at 110°C. Free amino acids were converted to the fluorescent derivative DABS-AA (dimethylaminoazobenzene sulphonyl amino acids) and the total amino acid content was determined by HPLC with a fluorescence detector, thus the protein content was evaluated. The results of this determination indicated that the protein content in the sample was less than 0.54%.

A solution of lambda DNA–Hind III was diluted to ~0.05 mg/ml and heated over its T_m point at 100°C for 15 min, then cooled down quickly to 0°C. About 4 µl of the treated solution was deposited on to a freshly cleaved graphite surface and dried in air.

RESULTS AND DISCUSSION

It was found that most of the STM images of denatured DNA showed random coiling of the strands, while others showed conformations of multiple strands which were hard to be clearly identified. However, some highly ordered regions were found which provide new insight into the conformations of the denatured DNA.

Figures 1(a) and 1(b) show the constant current topographic image and barrier-height image, respectively, acquired simultaneously on freshly cleaved graphite with some surface features. Figures 2(a) and 2(b) show the STM topographic image of the denatured DNA and corresponding barrier-height image, respectively. The experimental conditions were the same for Figures 1 and 2. Despite the fact that resolution of the barrier-height image of Figure 2(b) is not as good as that of the topographic image of Figure 2(a), it is obvious that similar corrugations can be seen in both images. In contrast, no remarkable corrugations

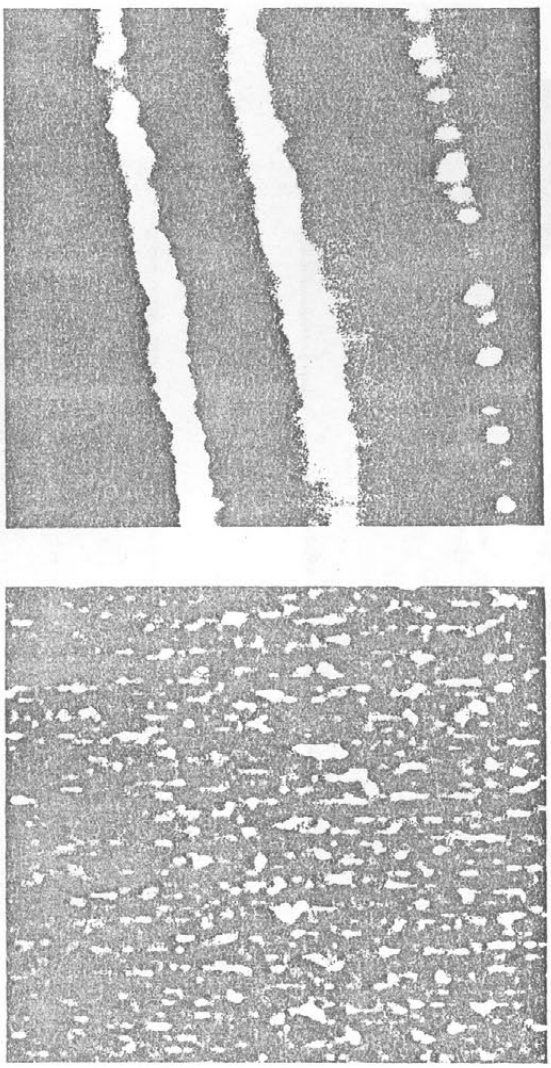

(*a*)

(*b*)

FIGURE 1. (a) STM image (4.3 × 4.6 nm) of freshly cleaved graphite with surface features. STM was operated with a tip bias of 16 mV and a feedback system maintaining a current of 0.6 nA. (b) The corresponding barrier-height image.

have emerged in the barrier-height image of Figure 1(b). A strong d*I*/d*S* signal the DNA molecule in Figure 2(b) indicates a profound difference in barrier-height between the DNA and the HOPG substrate.

We believe that the STM image shown in Figure 2(a) is an adsorbed DNA molecule rather than an artefact of the substrate because of the following considerations. We have found that the STM topographic images of freshly cleaved graphite on which no biomaterials were deposited showed large atomically flat areas with some inherent features (Figure 1(a)) which may be confused with DNA molecules, but the corresponding barrier-height images acquired simultaneously appeared practically featureless (Figure 1(b)). In other words, the regular periodicities along the step edges of graphite presented in the topographic

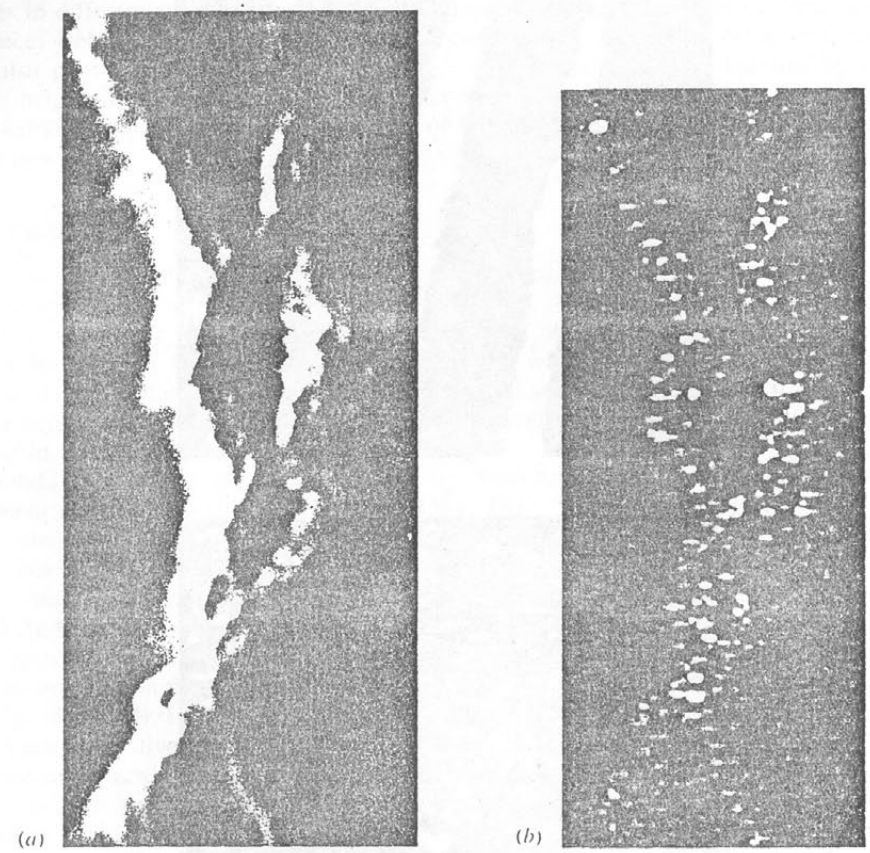

FIGURE 2. (a) STM image (2.0 × 4.8 nm) of two zig-zag-like double-stranded segments crossing at one point. Experimental conditions were the same as those in Figure 1. (b) The corresponding barrier-height image.

image did not appear in the barrier-height images acquired simultaneously as long as the experimental parameters were appropriate. However, similar corrugations are present in both topographic and barrier-height images over DNA under the same conditions as those used for imaging bare graphite. Similar results have also been obtained by Travaglini *et al.* (1987) and Driscoll *et al.* (1990). As they pointed out, on relatively rigid surfaces such as graphite surface, d*I*/d*S* is a measure of the average tunneling barrier-height – an increase in the value of the barrier-height usually indicates the presence of excess negative surface charge. For a low bias voltage (~ 15 mV) and tunneling current (~ 0.5 nA), deformation of the graphite surface induced by the tip of should not be important, which makes the barrier-height image of graphite appear practically structureless. On 'soft' surface such as the adsorbed biological materials, forces of inter-atomic and Coulombic nature between the tip and the surface enhance d*I*/d*S* when attractive, and reduce it when repulsive. Thus, while the tip is scanning across DNA molecules, similar corrugations will occur in both topographic and barrier-height images. Moreover, charging effects on the DNA molecules would be expected to occur because of their non-conductive nature. Thus, one would expect the barrier-height of the substrate in the vicinity of the adsorbed DNA to increase with

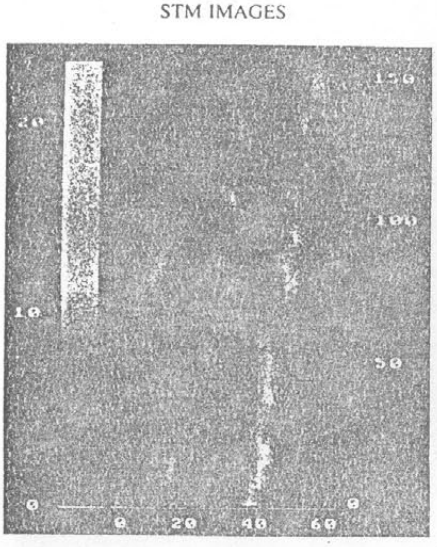

FIGURE 3. STM image of a joint structure between triple-stranded, braid-like section and right-handed double helical section. Experimental conditions were the same as those in Figure 1.

respect to bare substrate surrounding the molecule (Tarvaglini *et al.*, 1987). The barrier-height image shown in Figure 2(b) clearly shows this effect over the feature we identify as DNA. d*I*/d*S* measurements have also been used by Lindsay *et al.* (1988) to identify adsorbate patches of DNA electrochemically mounted on atomically flat gold surfaces and imaged in a liquid environment.

Figure 3 shows a braid-like conformation segment of denatured DNA with a width of about 3 nm, which can be interpreted as a triple-stranded helix in which two of the three strands first form a right-handed double helical conformation and then join the left strand to form the triple-stranded, braid-like conformation. Figure 4 shows another triple-stranded, braid-like chain with a width of 2.9 nm. Figure 5 shows the STM image of right-handed and left-handed double helices existing in one chain. The corresponding barrier-height images obtained simultaneously with the topographic images shown in Figures 3–5 are not presented for simplicity, but also show similar corrugations.

The results presented here indicate that STM can be applied to the study of the variant conformations of denatured DNA. A model of right-handed triple helical DNA has already been proposed (Arnott & Selsing, 1974; Arnott *et al.*, 1974, 1976; Gago & Richards, 1989; Moffat, 1991), which shows promise as a tool for cleaving genomes precisely and blocking gene transcription. We have observed the conformation of DNA (not shown here) which is quite close to the model, with the only exception that the observed structure is left-handed.

The existence of a triple-stranded, braid-like conformation of DNA has not been proposed before. The images of Figures 3 and 4 have shown clearly the existence of the segment of such braid-like conformations, which provide new insight into the conformations of denatured DNA. At present, little is known about how the triple-stranded, braid-like DNA is formed and what the possible function is, but this conformation can be explained by base-pairing. For such a braid-like conformation, the bases containing hydrogen bond interaction must adopt the forms of base triplets. Thirty-six kinds of possible base triplets including protonated cytosine and adenine have been derived as shown in Figure 6. The other triplets occupy the glycol bond, so they would not be involved in the braid-like conformation. These triplets can be formed in four ways, i.e. Watson–Crick–Hoogsteen, Watson–Crick–Reversed Hoogsteen, Reversed Watson–Crick–Hoogsteen and Reversed Watson–Crick–Reversed Hoogsteen. Among these, the middle bases must be purine bases

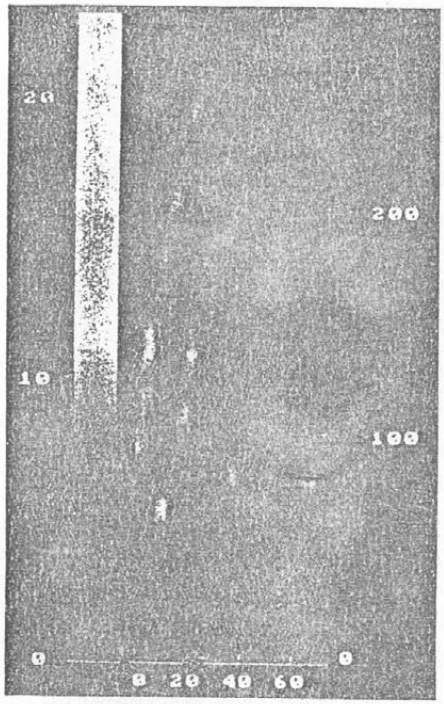

FIGURE 4. STM image (7.2 × 28.4 nm) of a single triple-stranded, braid-like chain. Experimental conditions were the same as those in Figure 1.

because pyrimidine bases do not have an imidazole ring. In these triplets, the Hoogsteen and Reversed Hoogsteen pairs can be formed by hydrogen bonding of the N7 on the imidazole ring with the proton donor on other bases. The calculated results of Pullman (Pullman & Pullman, 1969) and other authors showed that the interaction energy of the G–C pair formed in Watson–Crick way was minimized, but for A–U and A–T pairs, the interaction energies were minimized only when they were formed in the Hoogsteen, or Reversed Hoogsteen way. These conclusions are consistent with the experimental observation of co-crystallization phenomena. In the triple-helix DNA (Arnott & Selsing, 1974; Arnott *et al.*, 1976; Letai *et al.*, 1988; Htun & Dahlberg, 1989; Moffat, 1991), two strands must be pyrimidine bases and the middle one must be purine bases. The triple-stranded, braid-like conformation presented in this work is different from the triple helix just described, with its triple strands crossing together to form a braid-like chain. There is no requirement for any individual strand to be homopurine or homopyrimidine. However, each strand in the braid-like chain must contain repeating units of purine or pyrimidine which consists of A, G or A and G. Between the repeating units, there can be a purine nucleotide sequence, pyrimidine nucleotide sequence or a mixture of them. The detailed discussions will be published elsewhere.

Sasisekharan *et al.* (1978) have proposed a double-stranded model of an alternative structure for DNA, in which right- and left-handed helical segments with approximately five base pairs in length alternate in arrangement. The conformation of denatured DNA shown in Figure 5 is similar to this model.

Besides the secondary structures shown above, some different kinds of tertiary structures were also observed. Figure 2(a) presents two zig-zag-like double-stranded segments

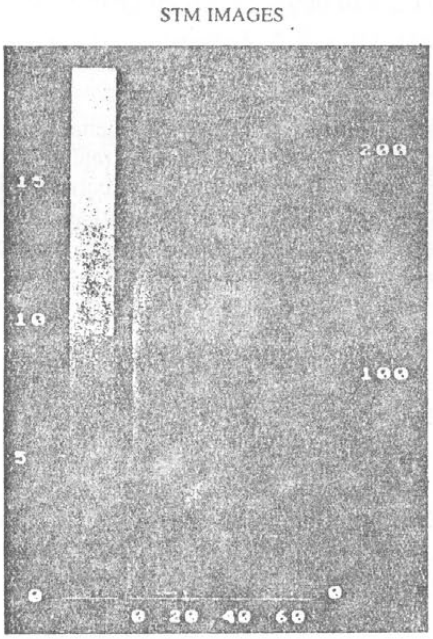

FIGURE 5. STM image of right-handed and left-handed double helices existing in one chain. Experimental conditions were the same as those in Figure 1.

CAC	CAC*	TAT	GAT	C*GA	TGC	GGG	M*GGC
TAC	TAC*	TAA	GAG	TGA	A*GC	A*GT	
GAC	GAC*	GAA	GGA	A*GA	C*GT	C*GG	
AAC	AAC*	AAA	GGC	C*GC	TGT	A*GG	
GTA	CGC	GCA	GGT	CGA	CGT	AGA	

FIGURE 6. Thirty-six kinds of possible base triplets including protonized cytosine and adenine.

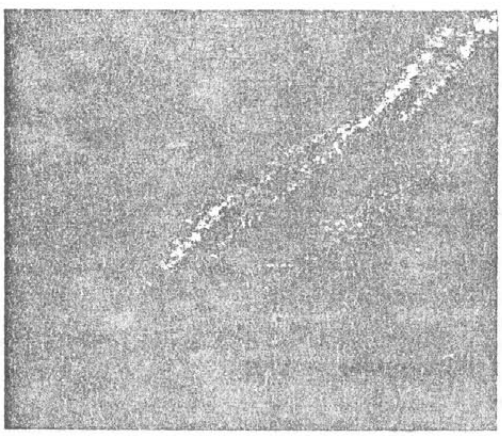

FIGURE 7. STM image of a supercoiled conformation consisted of two double helical DNA chains. Scanning area is 35 × 35 nm. Experimental conditions were the same as those in Figure 1.

crossing at one point. Figure 7 shows a supercoiled conformation consisting of two double helical DNA chains. We have also observed several kinds of spring-like tertiary structures.

CONCLUSIONS

In this paper we have presented some STM images of denatured lambda phage DNA–Hind III. In order to distinguish DNA molecules from substrate surface features which may be confused with the biological materials, topographic and barrier-height images were acquired simultaneously in the experiments. There were no remarkable features in the barrier-height images of the freshly cleaved graphite. However, similar features were appeared in both topographic and barrier-height images on DNA-treated graphite surfaces. Unusual triple-stranded, braid-like DNA, and joint structures of triple-stranded and double-stranded helical segments were imaged.

ACKNOWLEDGEMENTS

This work was supported by Chinese Academy of Sciences. We thank Professors John D. Baldeschwieler, D. Liang, C. Chen, Y. Tang and Dr Scott Gilbert for discussions. We also thank our colleagues F. Gao, G. Huang, H. Sun, P. Zhang and G. Liu *et al.* for their participating in the work of repetition of experiments, determination of the content of protein in the sample and development of computer software.

REFERENCES

ALLISON, D.P., THOMPSON, J.R., JACOBSON, K.B., WARMACK, R.J. & FERRELL, T.L. (1990) Scanning tunneling microscopy and spectroscopy of plasmid DNA. *Scanning Microscopy* **4**, 517–522.

ARNOTT, S. & SELSING, E. (1974) Structures for the polynucleotide complexes poly(dA) . poly(dT) and poly(dT) . poly(dA) . poly(dT). *Journal of Molecular Biology* **88**, 509–521.

ARNOTT, S., CHANDRASEKARAN, R., HUKINS, D.W.L., SMITH, P.J.C. & WATTS, L. (1974) Structural details of a double-helix observed for DNAs containing alternating purine and pyrimidine sequences. *Journal of Molecular Biology* **88**, 523–533.

ARNOTT, S., BOND, P.J., SELSING, E. & SMITH, P.J.C. (1976) Models of triple-stranded polynucleotides with optimised stereochemistry. *Nucleic Acids Research* **3**, 2459–2470.

ARSCOTT, P.G., LEE, G., BLOOMFIELD, V.A. & EVANS, D.F. (1989) Scanning tunnelling microscopy of Z-DNA. *Nature* **339**, 484–486.

BAI, C. (1989) Computer-controlled scanning tunneling microscope. *Chinese Science Bulletin* **34**, 1318–1320.

BEEBE, T.P., JR., WILSON, T.E., OGLETREE, D.F., KATZ, J.E., BALHORN, R., SALMERON, M.B. & SIEKHAUS, W. (1989) Direct observation of native DNA structures with the scanning tunneling microscope. *Science* **243**, 370–372.

CLEMMER, C.R. & BEEBE, T.P., JR. (1991) Graphite: a mimic for DNA and other biomolecules in STM studies. *Science* **251**, 640–642.

DRISCOLL, R.J., YOUNGQUIST, M.G. & BALDESCHWIELER, J.D. (1990) Atomic-scale imaging of DNA using scanning tunnelling microscopy. *Nature* **346**, 294–296.

DUNLAP, D.D. & BUSTAMANTE, C. (1989) Images of single-stranded nucleic acids by scanning tunnelling microscopy. *Nature* **342**, 204–206.

GAGO, F. & RICHARDS, W.G. (1989) One left-handed strand in DNA-oligonucleotide complexes? *FEBS Letters* **242**, 270–274.

HEUN, H. & DAHLBERG, J.E. (1989) Topology and formation of triple-stranded H-DNA. *Science* **243**, 1571–1576.

LEE, G., ARSCOTT, P.G., BLOOMFIELD, V.A. & EVANS, D.F. (1989) Scanning tunneling microscopy of nucleic acids. *Science* **244**, 475–477.

LETAI, A.G., PALLADINO, M.A., FROMM, E., RIZZO, V. & FRESCO, J.R. (1988) Specificity in formation of triple-stranded nucleic acid helical complexes: studies with agarose-linked polyribonucleotide affinity columns. *Biochemistry* **27**, 9108–9112.

LINDSAY, S.M. & BARRIS, B. (1988) Imaging deoxyribose nucleic acid molecules on a metal surface under water by scanning tunneling microscopy. *Journal of Vacuum Science and Technology*, **A6**, 544–547.

LINDSAY, S.M., THUNDAT, T., NAGAHARA, L., KNIPPING, U. & RILL, R.L. (1989) Images of the DNA double helix in water. *Science* **244**, 1063–1064.

MOFFAT, A.S. (1991) Triplex DNA finally comes of age. *Science* **252**, 1374–1375.

PULLMAN, B. & PULLMAN, A. (1969) *Process in Nucleic Acid Research and Molecular Biology* (DAVIDSON, J.N. *et al.*, Eds). Vol 9. Academic Press, New York, London, pp. 327–402.

SASISEKHARAN, V., PATTABIRAMAN, N. & GUPTA, G. (1978) Some implications of an alternative structure for DNA. *Proceedings of the National Academy of Sciences, USA* **75**, 4092–4096.

SOMMERFELD, D.A., CAMBRON, R.T. & BEEBE, T.P., JR. (1990) Topographic and diffusion measurements of gold and platinum surfaces by scanning tunneling microscopy. *Journal of Physical Chemistry* **94**, 8926–8932.

TARVAGLINI, G., ROHRER, H., AMREIN, M. & GROSS, H. (1987) Scanning tunneling microscopy on biological matter. *Surface Sciences* **181**, 380–390.